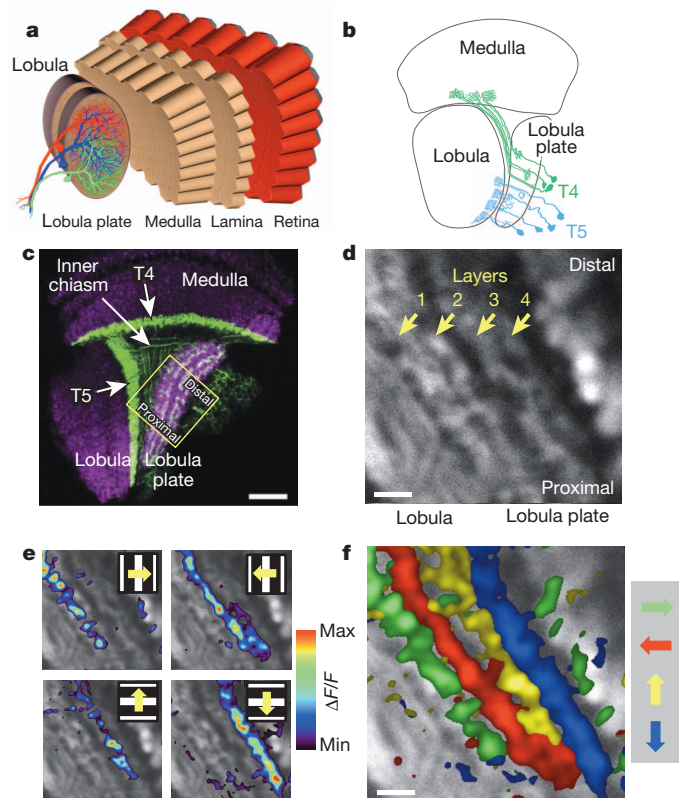


# A directional tuning map of *Drosophila* elementary motion detectors

Matthew S. Maisak<sup>1\*</sup>, Juergen Haag<sup>1\*</sup>, Georg Ammer<sup>1</sup>, Etienne Serbe<sup>1</sup>, Matthias Meier<sup>1</sup>, Aljoscha Leonhardt<sup>1</sup>, Tabea Schilling<sup>1</sup>, Armin Bahl<sup>1</sup>, Gerald M. Rubin<sup>2</sup>, Aljoscha Nern<sup>2</sup>, Barry J. Dickson<sup>3</sup>, Dierk F. Reiff<sup>1†</sup>, Elisabeth Hopp<sup>1</sup> & Alexander Borst<sup>1</sup>

The extraction of directional motion information from changing retinal images is one of the earliest and most important processing steps in any visual system. In the fly optic lobe, two parallel processing streams have been anatomically described, leading from two first-order interneurons, L1 and L2, via T4 and T5 cells onto large, wide-field motion-sensitive interneurons of the lobula plate<sup>1</sup>. Therefore, T4 and T5 cells are thought to have a pivotal role in motion processing; however, owing to their small size, it is difficult to obtain electrical recordings of T4 and T5 cells, leaving their visual response properties largely unknown. We circumvent this problem by means of optical recording from these cells in *Drosophila*, using the genetically encoded calcium indicator GCaMP5 (ref. 2). Here we find that specific subpopulations of T4 and T5 cells are directionally tuned to one of the four cardinal directions; that is, front-to-back, back-to-front, upwards and downwards. Depending on their preferred direction, T4 and T5 cells terminate in specific sublayers of the lobula plate. T4 and T5 functionally segregate with respect to contrast polarity: whereas T4 cells selectively respond to moving brightness increments (ON edges), T5 cells only respond to moving brightness decrements (OFF edges). When the output from T4 or T5 cells is blocked, the responses of postsynaptic lobula plate neurons to moving ON (T4 block) or OFF edges (T5 block) are selectively compromised. The same effects are seen in turning responses of tethered walking flies. Thus, starting with L1 and L2, the visual input is split into separate ON and OFF pathways, and motion along all four cardinal directions is computed separately within each pathway. The output of these eight different motion detectors is then sorted such that ON (T4) and OFF (T5) motion detectors with the same directional tuning converge in the same layer of the lobula plate, jointly providing the input to downstream circuits and motion-driven behaviours.

Most of the neurons in the fly brain are dedicated to image processing. The respective part of the head ganglion, called the optic lobe, consists of several layers of neuropile called lamina, medulla, lobula and lobula plate, all built from repetitive columns arranged in a retinotopic way (Fig. 1a). Each column houses a set of identified neurons that, on the basis of Golgi staining, have been described anatomically in great detail<sup>3–5</sup>. Owing to their small size, however, most of these columnar neurons have never been recorded from electrophysiologically. Therefore, their specific functional role in visual processing is still largely unknown. This fact is contrasted by rather detailed functional models about visual processing inferred from behavioural studies and recordings from the large, electrophysiologically accessible output neurons of the fly lobula plate (tangential cells). As the most prominent example of such models, the Reichardt detector derives directional motion information from primary sensory signals by multiplying the output from adjacent photoreceptors after asymmetric temporal filtering<sup>6</sup>. This model makes a number of rather counter-intuitive predictions all of which have been confirmed experimentally (for review, see ref. 7). Yet, the neurons corresponding to most



**Figure 1 | Directional tuning and layer-specific projection of T4 and T5 cells.** **a**, Schematic diagram of the fly optic lobe. In the lobula plate, motion-sensitive tangential cells extend their large dendrites over many hundreds of columns. Shown are the reconstructions of the three cells of the horizontal system<sup>22</sup>. **b**, Anatomy of T4 and T5 cells, as drawn from Golgi-impregnated material (from ref. 5). **c**, Confocal image of the Gal4-driver line R42F06, shown in a horizontal cross-section (from ref. 10). Neurons are marked in green (Kir2.1-EGFP labelled), whereas the neuropile is stained in purple by an antibody against the postsynaptic protein Dlg. Scale bar, 20  $\mu$ m. **d**, Two-photon image of the lobula plate of a fly expressing GCaMP5 under the control of the same driver line R42F06. Scale bar, 5  $\mu$ m. The size and orientation of the image approximately corresponds to the yellow square in **c**. **e**, Relative fluorescence changes ( $\Delta F/F$ ) obtained during 4-s grating motion along the four cardinal directions, overlaid on the grayscale image. Each motion direction leads to activity in a different layer. Minimum and maximum  $\Delta F/F$  values were 0.3 and 1.0 (horizontal motion), and 0.15 and 0.6 (vertical motion). **f**, Compound representation of the results obtained from the same set of experiments. Scale bar, 5  $\mu$ m. Results in **e** and **f** represent the data obtained from a single fly averaged over four stimulus repetitions. Similar results were obtained from six other flies.

<sup>1</sup>Max Planck Institute of Neurobiology, 82152 Martinsried, Germany. <sup>2</sup>Janelia Farm Research Campus, Ashburn, Virginia 20147, USA. <sup>3</sup>Institute of Molecular Pathology, 1030 Vienna, Austria. <sup>†</sup>Present address: Institute Biology 1, Albert-Ludwigs University, 79085 Freiburg, Germany.

\*These authors contributed equally to this work.

of the circuit elements of the Reichardt detector have not been identified so far. Here, we focus on a set of neurons called T4 and T5 cells (Fig. 1b) which, on the basis of circumstantial evidence, have long been speculated to be involved in motion detection<sup>1,8–10</sup>. However, it is unclear to what extent T4 and T5 cells are directionally selective or whether direction selectivity is computed or enhanced within the dendrites of the tangential cells. Another important question concerns the functional separation between T4 and T5 cells; that is, whether they carry equivalent signals, maybe one being excitatory and the other inhibitory on the tangential cells, or whether they segregate into directional- and non-directional pathways<sup>11</sup> or into separate ON- and OFF-motion channels<sup>12,13</sup>.

To answer these questions, we combined Gal4-driver lines specific for T4 and T5 cells<sup>14</sup> with GCaMP5 (ref. 2) and optically recorded the visual response properties using two-photon fluorescence microscopy<sup>15</sup>. In a first series of experiments, we used a driver line labelling both T4 and T5 cells. A confocal image (Fig. 1c, modified from ref. 10) revealed clear labelling (in green) in the medulla (T4 cell dendrites), in the lobula (T5 cell dendrites), as well as in four distinct layers of the lobula plate, representing the terminal arborizations of the four subpopulations of both T4 and T5 cells. These four layers of the lobula plate can also be seen in the two-photon microscope when the calcium indicator GCaMP5 is expressed (Fig. 1d). After stimulation of the fly with grating motion along four cardinal directions (front-to-back, back-to-front, upwards and downwards), activity is confined to mostly one of the four layers, depending on the direction in which the grating is moving (Fig. 1e). The outcome of all four stimulus conditions can be combined into a single image by assigning a particular colour to each pixel depending on the stimulus direction to which it responded most strongly (Fig. 1f). From these experiments it is clear that the four subpopulations of T4 and T5 cells produce selective calcium signals depending on the stimulus direction, in agreement with previous deoxyglucose labelling<sup>8</sup>. Sudden changes of the overall luminance evokes no responses in any of the layers (field flicker;  $n = 4$  experiments, data not shown). However, gratings flickering in counter-phase lead to layer-specific responses, depending on the orientation of the grating (Supplementary Fig. 1).

The retinotopic arrangement of this input to the lobula plate is demonstrated by experiments where a dark edge was moved within a small area of the visual field only. Depending on the position of this area, activity of T4 and T5 cells is confined to different positions within the lobula plate (Fig. 2a). Consequently, when moving a bright vertical edge horizontally from back to front, activity of T4 and T5 cells is elicited sequentially in layer 2 of the lobula plate (Fig. 2b). These two experiments also demonstrate that T4 and T5 cells indeed signal motion locally. We next investigated the question of where direction selectivity of T4 and T5 cells arises; that is, whether it is already present in the dendrite, or whether it is generated by synaptic interactions within the lobula plate. This question is hard to answer, as the dendrites of both T4 and T5 cells form a dense mesh within the proximal layer of the medulla (T4) and the lobula (T5), respectively. However, signals within the inner chiasm where individual processes of T4 and T5 cells can be resolved in some preparations show a clear selectivity for motion in one over the other directions (Fig. 2c). Such signals are as directionally selective as the ones measured within the lobula plate, demonstrating that the signals delivered from the dendrites of T4 and T5 cells are already directionally selective.

To assess the particular contribution of T4 and T5 cells to the signals observed in the above experiments, we used driver lines specific for T4 and T5 cells, respectively. Applying the same stimulus protocol and data evaluation as in Fig. 1, identical results were obtained as before for both the T4- as well as the T5-specific driver line (Fig. 3a, b). We conclude that T4 and T5 cells each provide directionally selective signals to the lobula plate, in contrast to previous reports<sup>11</sup>. Thus, both T4 and T5 cells can be grouped, according to their preferred direction, into four subclasses covering all four cardinal directions, reminiscent of ON–OFF ganglion cells of the rabbit retina<sup>16</sup>.

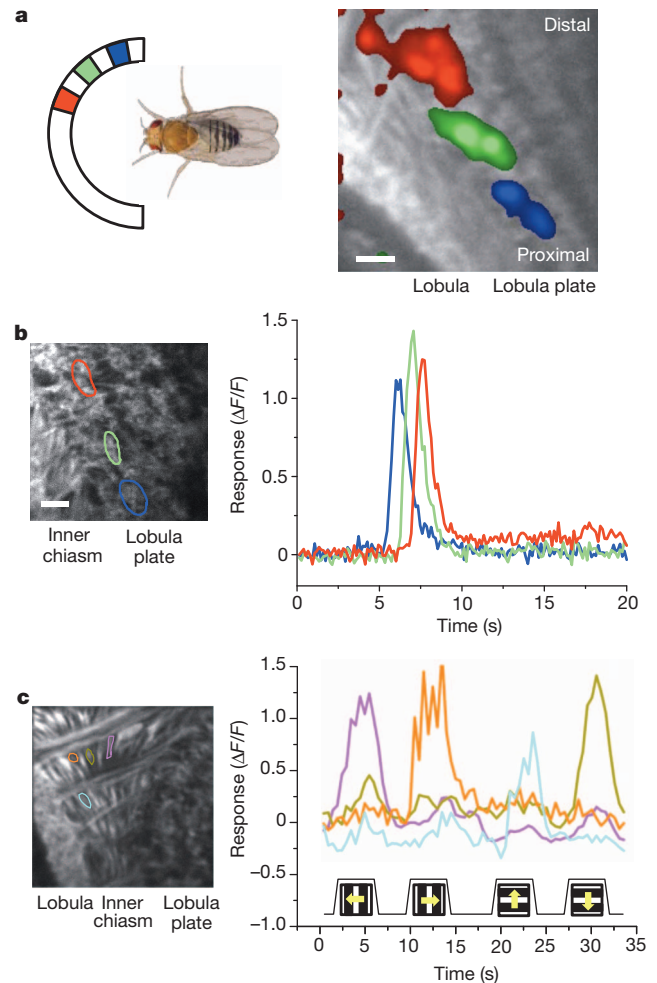


**Figure 2 | Local signals of T4 and T5 cells.** **a**, Retinotopic arrangement of T4 and T5 cells. A dark edge was moving repeatedly from front-to-back within a  $15^\circ$  wide area at different azimuthal positions (left). This leads to relative fluorescence changes at different positions along the proximal–distal axis within layer 1 of the lobula plate (right). Scale bar,  $5\ \mu\text{m}$ . Similar results have been obtained in four other flies. **b**, Sequential activation of T4 and T5 cells. A bright edge was moving from back-to-front at  $15^\circ\ \text{s}^{-1}$ . Scale bar,  $5\ \mu\text{m}$ . Similar results have been obtained in six other flies. **c**, Signals recorded from individual fibres within the inner chiasm (left) reveal a high degree of direction selectivity (right). Scale bar,  $5\ \mu\text{m}$ . Similar results were obtained from four other flies, including both lines specific for T4 and T5 cells. Response traces in **b** and **c** are derived from the region of interest encircled in the image with the same colour.

We next addressed whether T4 cells respond differently to T5 cells. To answer this question, we used, instead of gratings, moving edges with either positive (ON edge, brightness increment) or negative (OFF edge, brightness decrement) contrast polarity as visual stimuli. We found that T4 cells strongly responded to moving ON edges, but showed little or no response to moving OFF edges (Fig. 3c). This is true for T4 cells terminating in each of the four layers. We found the opposite for T5 cells. T5 cells selectively responded to moving OFF edges and mostly failed to respond to moving ON edges (Fig. 3d). Again, we found this for T5 cells in each of the four layers. We next addressed whether there are any other differences in the response properties between T4 and T5 cells by testing the velocity tuning of both cell populations by means of stimulating flies with grating motion along the horizontal axis from the front to the back at various velocities covering two orders of magnitude. T4 cells revealed a maximum response at a stimulus velocity of  $30^\circ\ \text{s}^{-1}$ , corresponding to a temporal frequency of 1 Hz (Fig. 3e). T5 cell responses showed a similar dependency on stimulus velocity, again with a peak at a temporal frequency of



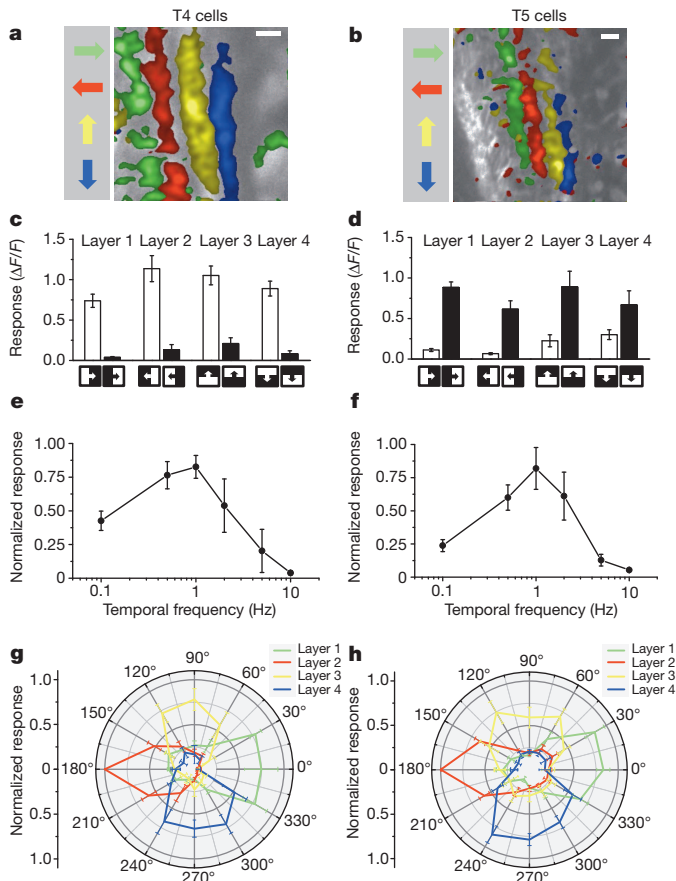


**Figure 3 | Comparison of visual response properties between T4 and T5 cells.** **a, b**, Relative fluorescence changes ( $\Delta F/F$ ) of the lobula plate terminals of T4 (**a**) and T5 (**b**) cells obtained during grating motion along the four cardinal directions. Results represent the data obtained from a single fly each, averaged over two stimulus repetitions. Scale bars, 5  $\mu\text{m}$ . Similar results have been obtained in ten other flies. **c, d**, Responses of T4 (**c**) and T5 (**d**) cells to ON and OFF edges moving along all four cardinal directions. ON (white) and OFF (black) responses within each layer are significantly different from each other, with  $P < 0.005$  except for layers 3 and 4 in T5 cells, where  $P < 0.05$ . **e, f**, Responses of T4 (**e**) and T5 (**f**) cells to gratings moving horizontally at different temporal frequencies. Relative fluorescence changes were evaluated from layer 1 of the lobula plate and normalized to the maximum response before averaging. **g, h**, Responses of T4 (**g**) and T5 (**h**) cells to gratings moving in 12 different directions. Relative fluorescence changes were evaluated from all four layers of the lobula plate normalized to the maximum response before averaging. Data represent the mean  $\pm$  s.e.m. of the results obtained in  $n = 8$  (**c**),  $n = 7$  (**d**),  $n = 6$  (**e**),  $n = 7$  (**f**),  $n = 6$  (**g**) and  $n = 5$  (**h**) different flies. Significances indicated are based on two-sample  $t$ -test.

1 Hz (Fig. 3f). Thus, there is no obvious difference in the velocity tuning between T4 and T5 cells. As another possibility, T4 cells might functionally differ from T5 cells with respect to their directional tuning width. To test this, we stimulated flies with gratings moving into 12 different directions and evaluated the relative change of fluorescence in all four layers of the lobula plate. Using the T4-specific driver line, we found an approximate half width of 60–90° of the tuning curve, with the peak responses in each layer shifted by 90° (Fig. 3g). No decrease of calcium was detectable for grating motion opposite to the preferred direction of the respective layer. When we repeated the experiments using the T5-specific driver line, we found a similar dependence of the relative change of fluorescence on the stimulus direction (Fig. 3h). We conclude that T4 cells have the same velocity and orientation tuning as T5 cells. The only functional difference we were able to detect remains their selectivity for contrast polarity.

Our finding about the different preference of T4 and T5 cells for the polarity of a moving contrast makes the strong prediction that selective

blockade of T4 or T5 cells should selectively compromise the responses of downstream lobula plate tangential cells to either ON or OFF edges. To test this prediction, we blocked the output of either T4 or T5 cells via expression of the light chain of tetanus toxin<sup>17</sup> and recorded the responses of tangential cells via somatic whole-cell patch to moving ON and OFF edges. In response to moving ON edges, strong and reliable directional responses were observed in all control flies (Fig. 4a). However, T4-block flies showed a strongly reduced response to ON edges, whereas the responses of T5-block flies were at the level of control flies (Fig. 4b, c). When we used moving OFF edges, control flies again responded with a large amplitude (Fig. 4d). However, the responses of T4-block flies were at the level of control flies, whereas the responses of T5-block flies were strongly reduced (Fig. 4e, f). These findings are reminiscent on the phenotypes obtained from blocking lamina cells L1 and L2 (ref. 13) and demonstrate that T4 and T5 cells are indeed the motion-coding intermediaries for these contrast polarities on their way to the tangential cells of the lobula plate. Whether the residual responses to ON edges in T4-block flies and to OFF edges in T5-block flies are due to an incomplete signal separation between the two pathways or due to an incomplete genetic block in both fly lines is currently unclear.

To address the question of whether T4 and T5 cells are the only motion detectors of the fly visual system, or whether they represent one cell class, in parallel to other motion-sensitive elements, we used tethered flies walking on an air-suspended sphere<sup>18</sup> and stimulated them by ON and OFF edges moving in opposite directions<sup>19</sup>. As in the previous experiments, we blocked T4 and T5 cells specifically by selective expression of the light chain of tetanus toxin. During balanced motion, control flies did not show significant turning responses to either side (Fig. 4g). T4-block flies, however, strongly followed the direction of the moving OFF edges, whereas T5-block flies followed the direction of the moving ON edges (Fig. 4h, i). In summary, the selective preference of T4-block flies for OFF edges and of T5-block flies for ON edges not only corroborates our findings about the selective preference of T4 and T5 cells for different contrast polarities, but also demonstrates that the signals of T4 and T5 cells are indeed the major, if not exclusive, inputs to downstream circuits and motion-driven behaviours.

Almost a hundred years after T4 and T5 cells have been anatomically described<sup>3</sup>, this study reports their functional properties in a systematic way. Using calcium as a proxy for membrane voltage<sup>20</sup>, we found that both T4 and T5 cells respond to visual motion in a directionally selective manner and provide these signals to each of the four layers of the lobula plate, depending on their preferred direction. Both cell types show identical velocity and orientation tuning which matches the one of the tangential cells<sup>21,22</sup>. The strong direction selectivity of both T4 and T5 cells is unexpected, as previous studies had concluded that the high degree of direction selectivity of tangential cells is due to a push–pull configuration of weakly directional input with opposite preferred direction<sup>23,24</sup>. Furthermore, as the preferred direction of T4 and T5 cells matches the preferred direction of the tangential cells branching within corresponding layers, it is currently unclear which neurons are responsible for the null-direction response of the tangential cells. As for the functional separation between T4 and T5 cells, we found that T4 cells selectively respond to brightness increments, whereas T5 cells exclusively respond to moving brightness decrements. Interestingly, parallel ON and OFF motion pathways had been previously postulated on the basis of selective silencing of lamina neurons L1 and L2 (ref. 13). Studies using apparent motion stimuli to probe the underlying computational structure arrived at controversial conclusions: whereas some studies concluded that there was a separate handling of ON and OFF events by motion detectors<sup>12,25,26</sup>, others did not favour such a strict separation<sup>19,27</sup>. The present study directly demonstrates the existence of separate ON and OFF motion detectors, as represented by T4 and T5 cells, respectively. Furthermore, our results anatomically confine the essential processing steps of elementary

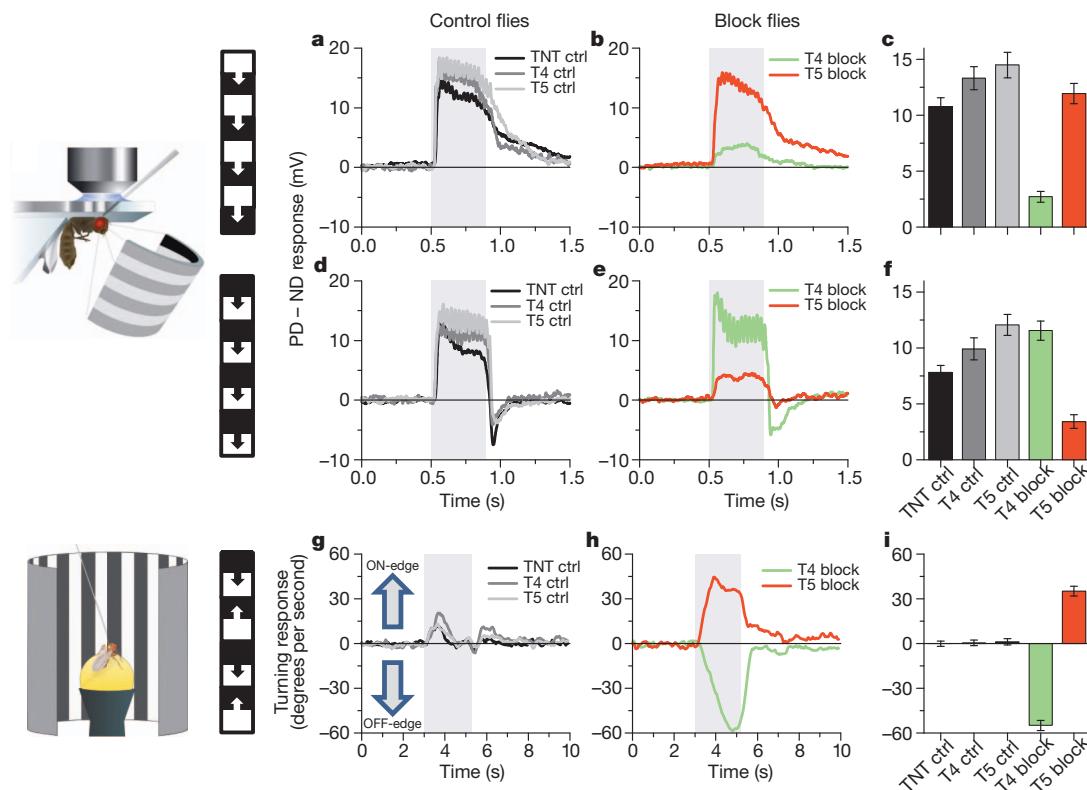


**Figure 4 | Voltage responses of lobula plate tangential cells and turning responses of walking flies to moving ON and OFF edges.** **a, d,** Average time course of the membrane potential in response to preferred direction motion minus the response to null direction motion (PD – ND response) as recorded in three types of control flies (stimulation period indicated by shaded area). **b, e,** Same as in **a, d**, but recorded in T4-block flies (green) and T5-block flies (red). The stimulus pattern, shown to the left, consisted of multiple ON- (**a**) or OFF-edges (**d**). **c, f,** Mean voltage responses (PD – ND) of tangential cells in the five groups of flies. Recordings were done from cells of the vertical<sup>21</sup> and the horizontal<sup>22</sup> system. Because no difference was detected between them, data were pooled. Data comprise recordings from  $n = 20$  (TNT control),  $n = 12$  (T4 control),  $n = 16$  (T5 control),  $n = 17$  (T4 block) and  $n = 18$  (T5 block) cells. In both T4 and T5-block flies, ON and OFF responses are significantly different

from each other with  $P < 0.001$ . In T4-block flies, ON responses are significantly reduced compared to all three types of control flies, whereas in T5-block flies, OFF responses are significantly reduced, both with  $P < 0.001$ . **g,** Average time course of the turning response of three types of control flies to ON and OFF edges moving simultaneously to opposite directions (stimulation period indicated by shaded area). **h,** Same as in **g**, but recorded from T4-block flies (green) and T5-block flies (red). **i,** Mean turning tendency ( $\pm$  s.e.m.) during the last second of the stimulation period averaged across all flies within each group. Data comprise average values obtained in  $n = 12$  (TNT controls),  $n = 11$  (T4 controls),  $n = 13$  (T5 controls),  $n = 13$  (T4 block) and  $n = 12$  (T5 block) flies. Values of T4 and T5-block flies are highly significantly different from zero with  $P < 0.001$ . Significances indicated are based on two-sample  $t$ -test.

motion detection—that is, asymmetric temporal filtering and non-linear interaction—to the neuropile between the axon terminals of lamina neurons L1 and L2 (ref. 28) and the dendrites of directionally selective T4 and T5 cells (Supplementary Fig. 2). The dendrites of T4 and T5 cells might well be the place where signals from neighbouring columns interact in a nonlinear way, similar to the dendrites of starburst amacrine cells of the vertebrate retina<sup>29</sup>.

## METHODS SUMMARY

**Flies.** Flies used in calcium imaging experiments (Figs 1–3) had the following genotypes: T4/T5 line ( $w^-/+;$   $UAS-GCaMP5, R42F06-GAL4/UAS-GCaMP5, R42F06-GAL4$ ), T4 line ( $w^-/+;$   $UAS-GCaMP5, R54A03-GAL4/UAS-GCaMP5, R54A03-GAL4$ ), T5 line ( $w^-/+;$   $UAS-GCaMP5, R42H07-GAL4/UAS-GCaMP5, R42H07-GAL4$ ). Flies used in electrophysiological and behavioural experiments (Fig. 4) had identical genotypes of the following kind: TNT control flies ( $w^+/w^+;$   $UAS-TNT-E/UAS-TNT-E/+;$ ), T4 control flies ( $w^+/w^-;$   $+/+;$   $VT37588-GAL4/+;$ ), T5 control flies ( $w^+/w^-;$   $+/+;$   $R42H07-GAL4/+;$ ), T4-block flies ( $w^+/w^-;$   $UAS-TNT-E/+;$   $VT37588-GAL4/+;$ ), T5-block flies ( $w^+/w^-;$   $UAS-TNT-E/+;$   $R42H07-GAL4/+;$ ).

**Two-photon microscopy.** We used a custom-built two-photon laser scanning microscope<sup>29</sup> equipped with a  $\times 40$  water immersion objective and a mode locked Ti:sapphire laser. To shield the photomultipliers from the stimulus light, two separate barriers were used: the first was placed directly over the LEDs, the second extended from the fly holder over the arena. Images were acquired at a resolution of  $256 \times 256$  pixels and a frame rate of 1.87 Hz, except where indicated, using ScanImage software<sup>30</sup>.

**Electrophysiology.** Recordings were established under visual control using a Zeiss Microscope and a  $\times 40$  water immersion objective.

**Behavioural analysis.** The locomotion recorder was custom-designed according to ref. 18. It consisted of an air-suspended sphere floating in a bowl-shaped sphere holder. Motion of the sphere was recorded by two optical tracking sensors.

**Visual stimulation.** For calcium imaging and electrophysiological experiments, we used a custom-built LED arena covering  $180^\circ$  and  $90^\circ$  of the visual field along the horizontal and the vertical axis, respectively, at  $1.5^\circ$  resolution. For the behavioural experiments, three 120-Hz LCD screens formed a U-shaped visual arena with the fly in the centre, covering  $270^\circ$  and  $114^\circ$  of the visual field along the horizontal and the vertical axes, respectively, at  $0.1^\circ$  resolution.

**Data evaluation.** Data were evaluated off-line using custom-written software (Matlab and IDL).

**Full Methods** and any associated references are available in the online version of the paper.

Received 16 April; accepted 20 May 2013.

1. Bausenwein, B., Dittrich, A. P. M. & Fischbach, K. F. The optic lobe of *Drosophila melanogaster* II. Sorting of retinotopic pathways in the medulla. *Cell Tissue Res.* **267**, 17–28 (1992).
2. Akerboom, J. et al. Optimization of a GCaMP calcium indicator for neural activity imaging. *J. Neurosci.* **32**, 13819–13840 (2012).
3. Cajal, S. R. & Sanchez, D. *Contribucion al conocimiento de los centros nerviosos de los insectos* (Imprenta de Hijos de Nicholas Moja, 1915).
4. Strausfeld, N. J. *Atlas of an Insect Brain* (Springer, 1976).
5. Fischbach, K. F. & Dittrich, A. P. M. The optic lobe of *Drosophila melanogaster*. I. A Golgi analysis of wild-type structure. *Cell Tissue Res.* **258**, 441–475 (1989).

6. Reichardt, W. Autocorrelation, a principle for the evaluation of sensory information by the central nervous system. In *Sensory Communication* (ed. Rosenblith, W. A.) 303–317 (MIT Press and John Wiley & Sons, 1961).
7. Borst, A., Haag, J. & Reiff, D. F. Fly motion vision. *Annu. Rev. Neurosci.* **33**, 49–70 (2010).
8. Buchner, E., Buchner, S. & Buelthoff, I. Deoxyglucose mapping of nervous activity induced in *Drosophila* brain by visual movement. 1. Wildtype. *J. Comp. Physiol.* **155**, 471–483 (1984).
9. Strausfeld, N. J. & Lee, J. K. Neuronal basis for parallel visual processing in the fly. *Vis. Neurosci.* **7**, 13–33 (1991).
10. Schnell, B., Raghu, V. S., Nern, A. & Borst, A. Columnar cells necessary for motion responses of wide-field visual interneurons in *Drosophila*. *J. Comp. Physiol. A* **198**, 389–395 (2012).
11. Douglass, J. K. & Strausfeld, N. J. Visual motion-detection circuits in flies: Parallel direction- and non-direction-sensitive pathways between the medulla and lobula plate. *J. Neurosci.* **16**, 4551–4562 (1996).
12. Franceschini, N., Riehle, A. & Le Nestour, A. Directionally selective motion detection by insect neurons. In *Facets of Vision* (ed. Stavenga, H.) 360–390 (Springer, 1989).
13. Joesch, M., Schnell, B., Raghu, S. V., Reiff, D. F. & Borst, A. ON and OFF pathways in *Drosophila* motion vision. *Nature* **468**, 300–304 (2010).
14. Pfeiffer, B. D. *et al.* Tools for neuroanatomy and neurogenetics in *Drosophila*. *Proc. Natl Acad. Sci. USA* **105**, 9715–9720 (2008).
15. Denk, W., Strickler, J. H. & Webb, W. W. Two-photon laser scanning fluorescence microscopy. *Science* **248**, 73–76 (1990).
16. Oyster, C. W. & Barlow, H. B. Direction-selective units in rabbit retina: distribution of preferred directions. *Science* **155**, 841–842 (1967).
17. Sweeney, S. T., Broadie, K., Keane, J., Niemann, H. & O’Kane, C. J. Targeted expression of tetanus toxin light chain in *Drosophila* specifically eliminates synaptic transmission and causes behavioral defects. *Neuron* **14**, 341–351 (1995).
18. Seelig, J. D. *et al.* Two-photon calcium imaging from head-fixed *Drosophila* during optomotor walking behavior. *Nature Methods* **7**, 535–540 (2010).
19. Clark, D. A., Bursztyn, L., Horowitz, M. A., Schnitzer, M. J. & Clandinin, T. R. Defining the computational structure of the motion detector in *Drosophila*. *Neuron* **70**, 1165–1177 (2011).
20. Egelhaaf, M. & Borst, A. Calcium accumulation in visual interneurons of the fly: Stimulus dependence and relationship to membrane potential. *J. Neurophysiol.* **73**, 2540–2552 (1995).
21. Joesch, M., Plett, J., Borst, A. & Reiff, D. F. Response properties of motion-sensitive visual interneurons in the lobula plate of *Drosophila melanogaster*. *Curr. Biol.* **18**, 368–374 (2008).
22. Schnell, B. *et al.* Processing of horizontal optic flow in three visual interneurons of the *Drosophila* brain. *J. Neurophysiol.* **103**, 1646–1657 (2010).
23. Borst, A. & Egelhaaf, M. Direction selectivity of fly motion-sensitive neurons is computed in a two-stage process. *Proc. Natl Acad. Sci. USA* **87**, 9363–9367 (1990).
24. Single, S., Haag, J. & Borst, A. Dendritic computation of direction selectivity and gain control in visual interneurons. *J. Neurosci.* **17**, 6023–6030 (1997).
25. Eichner, H., Joesch, M., Schnell, B., Reiff, D. F. & Borst, A. Internal structure of the fly elementary motion detector. *Neuron* **70**, 1155–1164 (2011).
26. Joesch, M., Weber, F., Eichner, H. & Borst, A. Functional specialization of parallel motion detection circuits in the fly. *J. Neurosci.* **33**, 902–905 (2013).
27. Egelhaaf, M. & Borst, A. Are there separate ON and OFF channels in fly motion vision? *Vis. Neurosci.* **8**, 151–164 (1992).
28. Takemura, S. Y., Lu, Z. & Meinertzhagen, I. A. Synaptic circuits of the *Drosophila* optic lobe: the input terminals to the medulla. *J. Comp. Neurol.* **509**, 493–513 (2008).
29. Euler, T., Detwiler, P. B. & Denk, W. Directionally selective calcium signals in dendrites of starburst amacrine cells. *Nature* **418**, 845–852 (2002).
30. Pologruto, T. A., Sabatini, B. L. & Svoboda, K. ScanImage: Flexible software for operating laser scanning microscopes. *Biomed. Eng. Online* **2**, 13 (2003).

**Supplementary Information** is available in the online version of the paper.

**Acknowledgements** We thank L. Looger, J. Simpson, V. Jayaraman and the Janelia GECI team for making and providing us with the GCaMP5 flies before publication; J. Plett for designing and engineering the LED arena; C. Theile, W. Essbauer and M. Sauter for fly work; and A. Mauss, F. Gabbiani and T. Bonhoeffer for critically reading the manuscript. This work was in part supported by the Deutsche Forschungsgemeinschaft (SFB 870). M.S.M., G.A., E.S., M.M., A.L., A.Ba and A.Bo are members of the Graduate School of Systemic Neurosciences.

**Author Contributions** M.S.M. and J.H. jointly performed and, together with A.Bo., evaluated all calcium imaging experiments. G.A., E.S. and M.M. recorded from tangential cells. A.L., T.S. and A.Ba. performed the behavioural experiments. G.R., B.D. and A.N. generated the driver lines and characterized their expression pattern. D.F.R. performed preliminary imaging experiments. E.H. helped with programming and developed the PMT shielding for the two-photon microscope. A.Bo. designed the study and wrote the manuscript with the help of all authors.

**Author Information** Reprints and permissions information is available at [www.nature.com/reprints](http://www.nature.com/reprints). The authors declare no competing financial interests. Readers are welcome to comment on the online version of the paper. Correspondence and requests for materials should be addressed to A.Bo. ([borst@neuro.mpg.de](mailto:borst@neuro.mpg.de)).



## METHODS

**Flies.** Flies were raised on standard cornmeal-agar medium at 25 °C and 60% humidity throughout development on a 12 h light/12 h dark cycle. For calcium imaging, we used the genetically encoded single-wavelength indicator GCaMP5, variant G, with the following mutations: T302L, R303P and D380Y (ref. 2). Expression of GCaMP5 was directed by three different Gal4 lines, all from the Janelia Farm collection<sup>14</sup>. Flies used in calcium imaging experiments (Figs 1–3) had the following genotypes: T4/T5 line ( $w^-/+;$  *UAS-GCaMP5,R42F06-GAL4/UAS-GCaMP5,R42F06-GAL4*), T4 line ( $w^-/+;$  *UAS-GCaMP5,R54A03-GAL4/UAS-GCaMP5,R54A03-GAL4*), T5 line ( $w^-/+;$  *UAS-GCaMP5,R42H07-GAL4/UAS-GCaMP5,R42H07-GAL4*). All driver lines were generated by the methods described in ref. 14 and were identified by screening a database of imaged lines, followed by reimagining of selected lines<sup>31</sup>. As homozygous for both the Gal4-driver and the *UAS-GCaMP5* genes, T4 flies also showed some residual expression in T5 cells, and T5 flies also in T4 cells. This unspecific expression, however, was in general less than 25% of the expression in the specific cells. Flies used in electrophysiological and behavioural experiments (Fig. 4) had identical genotypes of the following kind: TNT control flies ( $w^+/w^+;$  *UAS-TNT-E/UAS-TNT-E*;  $+/+$ ), T4 control flies ( $w^+/w^-;$   $+/+$ ; *VT37588-GAL4/+*), T5 control flies ( $w^+/w^-;$   $+/+$ ; *R42H07-GAL4/+*), T4-block flies ( $w^+/w^-;$  *UAS-TNT-E/+*; *VT37588-GAL4/+*), T5-block flies ( $w^+/w^-;$  *UAS-TNT-E/+*; *R42H07-GAL4/+*). *UAS-TNT-E* flies were derived from the Bloomington Stock Center (stock no. 28837) and *VT37588-Gal4* flies were derived from the VDRC (stock no. 205893). Before electrophysiological experiments, flies were anaesthetized on ice and waxed on a Plexiglas holder using bees wax. The dissection of the fly cuticle and exposure of the lobula plate were performed as described previously (for imaging experiments, see ref. 32; for electrophysiology, see ref. 21). Flies used in behavioural experiments were taken from 18 °C just before the experiment and immediately cold-anaesthetized. The head, the thorax and the wings were glued to a needle using near-ultraviolet bonding glue (Sinfony Opaque Dentin) and strong blue LED light (440 nm, dental curing-light, New Woodpecker).

**Two-photon microscopy.** We used a custom-built two-photon laser scanning microscope<sup>33</sup> equipped with a  $\times 40$  water immersion objective (0.80 NA, IR-Achroplan; Zeiss). Fluorescence was excited by a mode locked Ti:sapphire laser ( $<100$  fs, 80 MHz, 700–1,020 nm; pumped by a 10 W CW laser; both Mai Tai; Spectraphysics) with a DeepSee accessory module attached for dispersion compensation control resulting in better pulse compression and fluorescence at the target sample. Laser power was adjusted to 10–20 mW at the sample, and an excitation wavelength of 910 nm was used. The photomultiplier tube (H10770PB-40, Hamamatsu) was equipped with a dichroic band-pass mirror (520/35, Brightline). Images were acquired at a resolution of  $256 \times 256$  pixels and a frame rate of 1.87 Hz, except in Fig. 2 (7.5 Hz), using the ScanImage software<sup>30</sup>.

**Electrophysiology.** Recordings were established under visual control using a  $\times 40$  water immersion objective (LumplanF, Olympus), a Zeiss microscope (Axiotech vario 100, Zeiss), and illumination (100 W fluorescence lamp, hot mirror, neutral density filter OD 0.3; all from Zeiss). To enhance tissue contrast, we used two polarization filters, one located as an excitation filter and the other as an emission filter, with slight deviation on their polarization plane. For eye protection, we additionally used a 420-nm LP filter on the light path.

**Behavioural analysis.** The locomotion recorder was custom-designed according to ref. 18. Briefly, it consists of an air-suspended sphere floating in a bowl-shaped sphere holder. A high-power infrared LED (800 nm, JET series, 90 mW, Roithner Electronics) is located in the back to illuminate the fly and the sphere surface. Two optical tracking sensors are equipped with lens and aperture systems to focus on the sphere behind the fly. The tracking data are processed at 4 kHz internally, read out via a USB interface and processed by a computer at  $\approx 200$  Hz. This allows real-time calculation of the instantaneous rotation axis of the sphere. A third camera (GRAS-20S4M-C, Point Grey Research) is located in the back which is essential for proper positioning of the fly and allows real-time observation and video recording of the fly during experiments.

**Visual stimulation.** For calcium imaging and electrophysiological experiments, we used a custom-built LED arena that allowed refresh rates of up to 550 Hz and 16 intensity levels. It covered  $180^\circ$  ( $1.5^\circ$  resolution) and  $90^\circ$  ( $1.5^\circ$  resolution) of the visual field along the horizontal and the vertical axis, respectively. The LED arena was engineered and modified based upon ref. 34. The LED array consists of  $7 \times 4$  individual TA08-81GWA dot-matrix displays (Kingbright), each harbouring  $8 \times 8$  individual green (568 nm) LEDs. Each dot-matrix display is controlled by an ATmega168 microcontroller (Atmel) combined with a ULN2804 line driver (Toshiba America) acting as a current sink. All panels are in turn controlled via an I2C interface by an ATmega128 (Atmel)-based main controller board, which reads in pattern information from a compact flash (CF) memory card. Matlab was used for programming and generation of the patterns as well as for sending the serial command sequences via RS-232 to the main controller board. The

luminance range of the stimuli was  $0.5\text{--}33\text{ cd m}^{-2}$ . For the calcium imaging experiments, two separate barriers were used to shield the photomultipliers from the stimulus light coming from the LED arena. The first was a spectral filter with transparency to wavelengths  $>540$  nm placed directly over the LEDs (ASF SFG 10, Microchemicals). The second was a layer of black PVC extending from the fly holder over the arena. Square wave gratings had a spatial wavelength of  $30^\circ$  of visual angle and a contrast of 88%. Unless otherwise stated, they were moving at  $30^\circ\text{ s}^{-1}$ . Edges had the same contrast and were also moving at  $30^\circ\text{ s}^{-1}$ . For the experiments shown in Figs 1, 2b and 3, each grating or edge motion was shown twice within a single sweep, resulting in a total of eight stimulation periods. Each stimulus period lasted 4 s, and subsequent stimuli were preceded by a 3-s pause. In the experiment shown in Fig. 2a, a dark edge of 88% contrast was moved for 1 s at  $15^\circ\text{ s}^{-1}$  from the front to the back at three different positions ( $22^\circ$ ,  $44^\circ$ ,  $66^\circ$ , from frontal to lateral). At each position, edge motion was repeated 15 times. For the experiment shown in Fig. 2b, a bright edge of 88% contrast was moving at  $15^\circ\text{ s}^{-1}$  from the back to the front, and images were acquired at a frame rate of 7.5 Hz. For the experiments shown in Figs 3e, f, all six stimulus velocities were presented once within one sweep, with the stimulus lasting 4 s, and different stimuli being separated by 2 s. In the experiments shown in Figs 3g, h, a single sweep contained all 12 grating orientations with the same stimulus and pause length as above. For the electrophysiology experiments (Fig. 4a–f), multiple edges were used as stimuli moving simultaneously at  $50^\circ\text{ s}^{-1}$ . To stimulate cells of horizontal system (HS cells), a vertical, stationary square-wave grating with  $45^\circ$  spatial wavelength was presented. For ON-edge motion, the right (preferred direction, PD) or the left edge (null direction, ND) of each light bar started moving until it merged with the neighbouring bar. For OFF-edge motion, the right or the left edge of each dark bar was moving. To stimulate cells of the vertical system (VS cells), the pattern was rotated by  $90^\circ$  clockwise. For the behavioural experiments (Fig. 4g–i), three 120-Hz LCD screens (Samsung 2233 RZ) were vertically arranged to form a U-shaped visual arena ( $w = 31\text{ cm} \times d = 31\text{ cm} \times h = 47\text{ cm}$ ) with the fly in the centre. The luminance ranged from 0 to  $131\text{ cd m}^{-2}$  and covered large parts of the flies' visual field (horizontal,  $\pm 135^\circ$ ; vertical,  $\pm 57^\circ$ ; resolution,  $<0.1^\circ$ ). The three LCD screens were controlled via NVIDIA 3D Vision Surround Technology on Windows 7 64-bit allowing a synchronized update of the screens at 120 frames per second. Visual stimuli were created using Panda3D, an open-source gaming engine, and Python 2.7, which simultaneously controlled the frame rendering in Panda3D, read out the tracking data and temperature and streamed data to the hard disk. The balanced motion stimulus consisted of a square-wave grating with  $45^\circ$  spatial wavelength and a contrast of 63%. Upon stimulation onset, dark and bright edges moved into opposite directions at  $10^\circ\text{ s}^{-1}$  for 2.25 s. This stimulation was performed for both possible edge directions and two initial grating positions shifted by half a wavelength, yielding a total of four stimulus conditions.

**Data evaluation.** Data were evaluated off-line using custom-written software (Matlab and IDL). For the images shown in Figs 1e, f, 2a and 3a, b, the raw image series was converted into four images representing the relative fluorescence change during each direction of grating motion:  $(\Delta F/F)_{\text{stim}} = (F_{\text{stim}} - F_{\text{ref}})/F_{\text{ref}}$ . The image representing the stimulus fluorescence ( $F_{\text{stim}}$ ) was obtained by averaging all images during stimulation; the image representing the reference fluorescence ( $F_{\text{ref}}$ ) was obtained by averaging three images before stimulation. Both images were smoothed using a Gaussian filter of 10 pixel half-width. For the images shown in Figs 1f and 3a, b,  $\Delta F/F$  images were normalized by their maximum value. Then, a particular colour was assigned to each pixel according to the stimulus direction during which it reached maximum value, provided it passed a threshold of 25%. Otherwise, it was assigned to background. The response strength of each pixel was coded as the saturation of that particular colour. For the data shown in Figs 2b, c and 3c–h, the raw image series was first converted into a  $\Delta F/F$  series by using the first three images as reference. Then, a region was defined within a raw image, and average  $\Delta F/F$  values were determined within that region for each image, resulting in a  $\Delta F/F$  signal over time. Responses were defined as the maximum  $\Delta F/F$  value reached during each stimulus presentation minus the average  $\Delta F/F$  value during the two images preceding the stimulus. For the bar graphs shown in Fig. 4c, f, the average voltage responses during edge motion (0.45 s) along the cell's preferred (PD) and null direction (ND) were calculated. For each recorded tangential cell, the difference between the PD and the ND response was determined, and these values were averaged across all recorded cells. The data shown in Fig. 4g, h were obtained from the four stimulus conditions by averaging the turning responses for the two starting positions of the grating and calculating the mean difference between the turning responses for the two edge directions. For the bar graph shown in Fig. 4i, the average turning response of each fly during the last second of balanced motion stimulation was calculated. These values were averaged across all recorded flies within each genotype.

31. Jenett, A. *et al.* A Gal4-driver line resource for *Drosophila* neurobiology. *Cell Rep.* **2**, 991–1001 (2012).
32. Reiff, D. F., Plett, J., Mank, M., Griesbeck, O. & Borst, A. Visualizing retinotopic half-wave rectified input to the motion detection circuitry of *Drosophila*. *Nature Neurosci.* **13**, 973–978 (2010).
33. Euler, T. *et al.* Eyecup scope—optical recording of light stimulus-evoked fluorescence signals in the retina. *Pflüger Arch.* **457**, 1393–1414 (2009).
34. Reiser, M. B. & Dickinson, M. H. A modular display system for insect behavioral neuroscience. *J. Neurosci. Methods* **167**, 127–139 (2008).

Copyright of Nature is the property of Nature Publishing Group and its content may not be copied or emailed to multiple sites or posted to a listserv without the copyright holder's express written permission. However, users may print, download, or email articles for individual use.